frontiers | Frontiers in Earth Science

TYPE Review
PUBLISHED 18 October 2024
DOI 10.3389/feart.2024.1488690

Check for updates

OPEN ACCESS

EDITED BY
Fuqiong Huang,
China Earthquake Networks Center, China

REVIEWED BY
Giovanni Martinelli,
National Institute of Geophysics and Volcanology, Italy
Guodong Zheng,
China University of Geosciences Wuhan, China

*CORRESPONDENCE
Hongbiao Gu,
hongbiaosw@126.com

RECEIVED 30 August 2024
ACCEPTED 08 October 2024
PUBLISHED 18 October 2024

CITATION
Li J, Liu Z, Chen Z, Gao Y, Hao Y and Gu H (2024) The role of gas emissions (He, Rn, and CO_2) from fault zones in understanding fault and seismic activity.
Front. Earth Sci. 12:1488690.
doi: 10.3389/feart.2024.1488690

The role of gas emissions (He, Rn, and CO_2) from fault zones in understanding fault and seismic activity

Jiye Li[1], Zhaofei Liu[2], Zhi Chen[2], Yan Gao[1], Yongmei Hao[1] and Hongbiao Gu[3]*

[1]Heilongjiang Earthquake Agency, Heilongjiang, China, [2]CEA Key Laboratory of Earthquake Prediction (Institute of Earthquake Forecasting), China Earthquake Administration, Beijing, China, [3]College of Transportation Engineering, Nanjing Tech University, Nanjing, China

Active fault zones are critical pathways for the migration of deep fluids to the Earth's surface, carrying gases such as He, Rn, and CO_2 that provide evidence for the physical and chemical dynamics of the Earth's interior. This review examines the geochemical characteristics of fault zone gases and their implications for understanding fault activity and seismic events. Fault zones with high activity levels exhibit significant gas release, and variations in soil and hot spring gas concentrations can serve as indicators of seismic activity. Changes in gas concentrations and isotopic ratios, particularly before and after earthquakes, reflect the dynamic interplay between deep-sourced and shallow-sourced fluids. Seismic-induced stress alterations enhance gas release along fault zones, leading to observable anomalies that can aid in earthquake monitoring and prediction. The study underscores the importance of isotope tracing in deciphering fluid sources, migration pathways, and the evolution of fault zones, providing valuable information for assessing tectonic activity and mitigating seismic risks.

KEYWORDS

gas emission, fault zone, fault activity, seismic activity, earthquake forecasting

1 Introduction

Fluids play a crucial role in Earth's system, particularly those migrating along fault zones, which often carry geochemical signatures indicating the physical and chemical evolution of Earth's deep interior. These fluids serve as valuable indicators for studying block movements, earthquake prediction, fault activity assessment, and related fields (Martinelli, 2020; Zhang et al., 2021). Due to the high permeability and porosity of active faults, these zones frequently act as conduits for the migration and release of deep-sourced fluids. This process typically manifests at the surface through elevated soil gas emissions, including radon (Rn), carbon dioxide (CO_2), helium (He), hydrogen (H_2), and methane (CH_4), as well as intense degassing from hot springs and increased geothermal heat flow (Weinlich, 2014; Voltattorni et al., 2015; Singh et al., 2016; Bond et al., 2017).

During fluid migration, stable isotope signatures of non-metallic elements frequently undergo equilibrium or kinetic fractionation. Isotopic analyses, such as $^{4}He/^{20}Ne$, $^{3}He/^{4}He$, and $\delta^{13}C_{CO2}$, can elucidate the origins, migration pathways, circulation processes, formation mechanisms, and evolutionary history of these fluids (Zheng et al., 2013;

Zhang et al., 2021). Furthermore, the chemical composition of fluids and isotopes is highly sensitive to variations in regional tectonic stress. Earthquake-induced stress changes can alter pore pressure and microcrack density, affecting fluid-rock interactions and subsequently modifying the surface emission levels of deep gases (Camarda et al., 2016; Randazzo et al., 2021; Caracausi et al., 2022). Therefore, analyzing the characteristics of fault zone gases and isotope sources provides an effective method for studying fluid migration within fault zones and its relationship to tectonic activity (Faulkner et al., 2010; Tian et al., 2021; Li et al., 2023).

2 Characteristics and sources of fluids in fault zones

2.1 Helium and neon

Helium (He) and neon (Ne) are inert noble gases whose isotopic compositions in various reservoirs make them effective geological tracers for mantle-derived fluids. Among the eight isotopic forms of helium, ^{3}He and ^{4}He are stable, while ^{5}He through ^{10}He are unstable. The ratios ^{4}He/^{20}Ne and ^{3}He/^{4}He are commonly employed to differentiate crustal from mantle-derived fluids (Sano and Wakita, 1985; Shao et al., 2024). The R/Ra ratio, representing He isotopic characteristics, is defined as the ratio of ^{3}He/^{4}He in a sample relative to that in the atmosphere.

In Earth's atmosphere, He is predominantly composed of ^{4}He, which constitutes ~99.99986% of atmospheric He. The concentration of He in the atmosphere is relatively low, at 5.239 ± 0.004 ppm (Walia et al., 2010). The atmospheric ^{3}He/^{4}He (Ra) value is 1.4×10^{-6}, and the ^{4}He/^{20}Ne value is ~0.318 (Sano and Wakita, 1985). Most atmospheric ^{4}He is radiogenic, originating from the α-decay of radioactive isotopes such as ^{238}U, ^{235}U, and ^{232}Th (Figure 1). The He abundance in Earth's crust is estimated at ~ 5.5×10^{-7}%. Crustal He typically exhibits an R/Ra value of ~0.02 and a ^{4}He/^{20}Ne value of 1,000 (Andrews, 1985). Conversely, the ^{3}He isotope, thought to originate from the solar nebula or solar wind radiation present during Earth's formation, has accumulated in the mantle throughout Earth's history. Mantle-derived He generally displays an R/Ra value exceeding 5 (Lupton, 1983), with mid-ocean ridge basalt (MORB) inclusions showing an R/Ra value of 8.0 and a ^{4}He/^{20}Ne value of 1,000 (Graham, 2002). R/Ra values between 5 and 50 are indicative of He from the lower mantle (White, 1957). The highest recorded R/Ra value of 67.2 ± 1.8 was found in olivine from 62 Ma-old lava flows on Baffin Island, suggesting a possible origin from Earth's core (Horton et al., 2023). Due to He's chemical inertness, stable physical properties, and low solubility in water, gases such as N_2 and CO_2, along with groundwater, often act as carriers for He migration (Hong et al., 2010; Walia et al., 2010; Lee et al., 2019). He typically accumulates in sedimentary basins and is released to the surface via faults or fractures (Gao et al., 2024).

2.2 Radon

Radon (Rn) is the only naturally occurring radioactive noble gas, existing in 34 unstable isotopic forms, ranging from ^{215}Rn to ^{242}Rn. In nature, radon is found primarily in three isotopes: ^{219}Rn (with a half-life of 3.96 s), ^{220}Rn (half-life of 55 s), and ^{222}Rn (half-life of 3.82 days) (Audi et al., 2003). Of these, ^{222}Rn is a decay product of ^{226}Ra in the ^{238}U decay chain (Figure 1), with the longest half-life, and its concentration in the atmosphere is typically ranging from 10 to 100 Bq·m^{-3} (Porstendörfer, 1994).

Uranium (U) and radium (Ra), naturally occurring radioactive elements, are widely distributed across the lithosphere, hydrosphere, and atmosphere. Uranium, which has 28 unstable isotopes (^{215}U to ^{242}U), is found in concentrations of ~3 $\times10^{-4}$% in the lithosphere and ~1 × 10^{-4}% in soil. Radium, with 33 unstable isotopes (^{202}Ra to ^{234}Ra), has lithospheric and soil concentrations of ~1 × 10^{-4}% and ~8×10^{-11}%, respectively (Cheng et al., 2005). The levels of U and Ra in soil or rock directly influence Rn release in soil gas (Pereira et al., 2017). Experimental studies on rock gas emissions have demonstrated that granite, which is rich in U and Ra, releases significantly higher Rn concentrations than limestone or sandstone (King, 1978; El-Arabi et al., 2006). Consequently, regions with extensive granite outcrops typically exhibit elevated Rn levels (Pereira et al., 2017).

Within mineral particles, radium undergoes α-decay, releasing α-particles (^{4}He) and enabling Rn to escape. The fraction of Rn atoms generated from the decay of ^{226}Ra that escape into rock pores is defined as the Rn emanation coefficient (Martinelli et al., 1995; Miklyaev et al., 2020; Phong Thu et al., 2020). Rn recoil can take three paths: 1) remaining within the same particle, 2) passing through a pore and embedding in adjacent particles, or 3) escaping into an open pore (Sakoda et al., 2011). Only Rn escaping into pore space is considered emanated (A, B, E, and F in Figure 2); otherwise, it is non-emanated (C, D, and G). The recoil range of Rn is 77 nm in water and 53 mm in the atmosphere, with the latter being 688 times greater (Sakoda et al., 2011). This difference indicates that rainfall and moisture content can significantly impact Rn diffusion.

Gas transport through porous media often occurs via two primary processes: diffusion and convection. Diffusion, driven by concentration gradients, involves the movement of substances from areas of high concentration to low concentration due to random molecular motion (Flügge and Zimens, 1939). Convection, also known as advection, mass transport, or viscous flow, is driven by pressure gradients (Ciotoli et al., 2007). In natural environments, gas transport typically results from a combination of these two mechanisms.

Due to Rn's relatively large atomic mass and chemical inertness, deep-source gases such as CO_2, N_2, and CH_4 often serve as carrier gases that facilitate its migration to the surface (Yuce et al., 2017). CO_2, the most prevalent component of Earth's interior, frequently acts as the carrier gas for Rn as it migrates along fault zones. Consequently, increased soil gas Rn concentrations are often observed in conjunction with rising CO_2 levels in fault zones (Li et al., 2013). In rock fractures and pores, typically ranging from 10^{-2} to 10^{1} mm in size at depths of several hundred to several thousand meters (Etiope and Martinelli, 2002; Girault and Perrier, 2014), Rn convection velocities can reach up to 10^{0} to 10^{4} m·d^{-1}(Etiope and Martinelli, 2002; Muto et al., 2021). For example, convection velocities of Rn in the Osaka Basin, Baikal Rift, and North Caucasus are estimated at 340 m·d^{-1}, 5.2 m·d^{-1}, and 28 m·d^{-1}, respectively

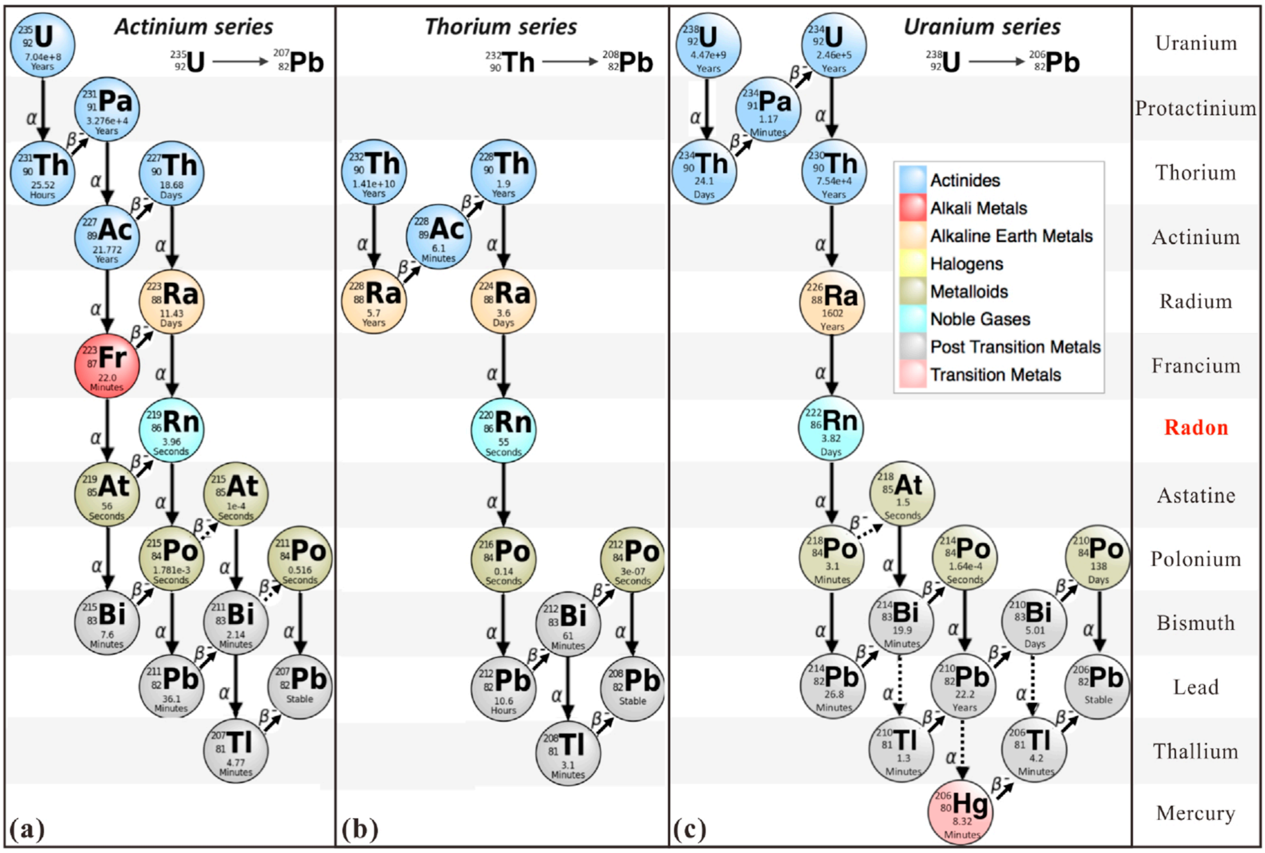

FIGURE 1
The α-decay chains of ^{219}Rn **(A)**, ^{220}Rn **(B)**, and ^{222}Rn **(C)**, adapted from Soddy (1913) and Tan (2016).

(Miklyaev et al., 2020; Muto et al., 2021). When CO_2 acts as the carrier gas, Rn may originate from depths of several hundred to several thousand meters in areas of high permeability (Girault and Perrier, 2014). Moreover, groundwater transport and deposition also contribute to the movement of Rn's parent elements, uranium, and radium (Chen et al., 2018).

2.3 Carbon dioxide

Data from the Mauna Loa Observatory in Hawaii proves that the CO_2 concentration in the atmosphere continues to increase, rising from 315.70 ppm in March 1958 to 422.80 ppm on 5 February 2024 (http://www.co2.earth). CO_2 primarily originates from three sources: the decomposition of organic material, the breakdown of carbonate rocks, and mantle degassing (Barnes et al., 1978). The origin of CO_2 can generally be determined using $\delta^{13}C_{CO2}$ values and CO_2 concentrations, which identify three distinct end-member sources: 1) Deep-source CO_2, derived from magmatic degassing and the decarbonation of carbonate rocks, typically exhibits concentrations near 100% with $\delta^{13}C_{CO2}$ values ~0‰ (Parks et al., 2013); 2) Biogenic CO_2, usually characterized by concentrations of ~4% and $\delta^{13}C_{CO2}$ values ~ −23‰ (Di Martino et al., 2016); and 3) Atmospheric CO_2, currently at 422.80 ppm, with $\delta^{13}C_{CO2}$ values ~ −8‰ (Keeling et al., 2005).

The range of $\delta^{13}C_{CO2}$ from different sources can overlap each other, such as those from Mid-Ocean Ridge Basalts (MORB) and carbonate rocks (Bergfeld et al., 2001). CO_2 also serves as the primary carrier gas for He migration in the crust (Hong et al., 2010; Walia et al., 2010; Lee et al., 2019). Therefore, the He-CO_2 system is often utilized to further deduce the source of CO_2 (Tian et al., 2021; Shao et al., 2024). Analysis of CO_2 origins can be conducted using R/Ra ratios and $\delta^{13}C_{CO2}$ values, which help distinguish between contributions from organic material, carbonate rock metamorphism, and mantle magma degassing (Barnes et al., 1978).

The decomposition of carbonate rocks involves processes such as water-rock interactions, mechanical grinding by faults, thermal metamorphism, and weathering (Rovira and Vallejo, 2008; Tamir et al., 2011). These processes can lead to the release of substantial amounts of CO_2, which then becomes a crustal fluid, potentially contaminating mantle-derived volatiles. Typically, thermal metamorphism of carbonate rocks occurs ~400°C; however, CO_2 release can begin at temperatures above 70°C when water is involved (Pankina G et al., 1979). Extensive fracture networks and fluid interactions can enhance water-rock reactions within the rock, producing significant quantities of CO_2 (Randazzo et al., 2021). Additionally, in regions of significant tectonic uplift, carbon stored in carbonate rocks for millions of years can be released through weathering (Zondervan et al., 2023).

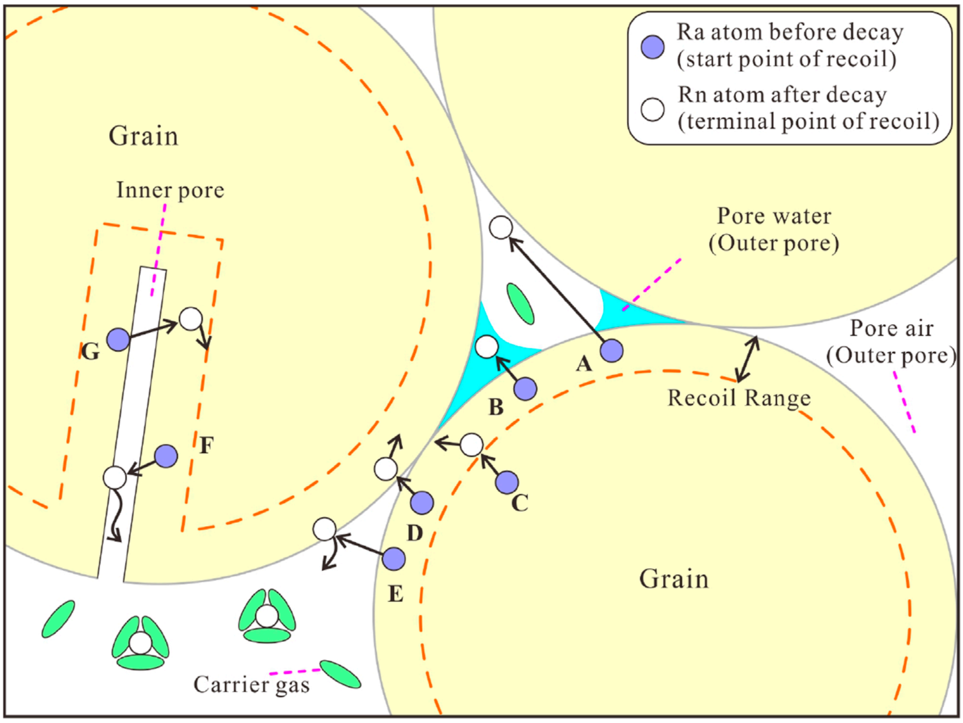

FIGURE 2
A schematic of Rn atom α-recoil, adapted from Sakoda et al. (2011). Arrows indicate diffusion processes, and the carrier gas is illustrative and does not represent actual behavior. **(A, B, E, F)** represent Rn emanated; **(C, D, G)** are non-emanated.

3 Application of fault zone gases in tectonic activity

The Earth is an open system where fluids, especially gaseous components, play a crucial role in material and energy exchange across different layers. Active fault systems, characterized by higher permeability and porosity, facilitate the migration of deep-seated fluids (such as CO_2 and He) toward the surface. These fault systems act as conduits extending to the mantle, allowing mantle-derived fluids to reach the Earth's surface. The geochemical signatures of these fluids provide valuable insights into the physicochemical evolution of the Earth's deep interior (Ciotoli et al., 2007; Yuce et al., 2017; Zhang et al., 2021), which constructed the major direction of gas geochemistry (Zheng et al., 2022). Therefore, in tectonically active regions, analyzing changes in fluid geochemical characteristics has become an essential method for studying block movements, earthquake prediction, revealing hidden faults, evaluating fault activity, and assessing atmospheric contributions (Zheng et al., 2018; Martinelli, 2020; Zhang et al., 2021).

3.1 Relationship between fault zone gases and tectonic activity

The exploration of soil gases, referred to as "geogas", dates back to 1913 (Klusman, 1993). Globally, regions of strong gas release often overlap with tectonic suture zones, volcanic belts, geothermal areas, and seismic zones (Barnes et al., 1978; Tamburello et al., 2018). Regionally, the intensity of fluid release and the geochemical characteristics within fault zones are closely related to fault activity. Significant anomalies in soil gas concentrations (such as Rn, CO_2, He, H_2, and CH_4) have been observed in various fault zones, including the Stivos Fault in Greece (Papastefanou, 2010), the Khlong Marui Fault in Thailand (Bhongsuwan et al., 2011), the Kütahya Simav Fault in Turkey (Manisa et al., 2022), and the Mat Fault in India (Jaishi et al., 2014). Field observations suggest that stronger fault activity correlates with increased soil gas release, making soil gas concentrations a useful metric for assessing fault activity (Seminsky et al., 2013; Capaccioni et al., 2015). Additionally, different fault types (normal, reverse, and strike-slip) exhibit distinct concentrations and flux characteristics (Annunziatellis et al., 2008; Sun et al., 2018). Therefore, tectonic zones with significant gas release are valuable for reconstructing regional geodynamic processes and monitoring subsurface tectonic activity (Faulkner et al., 2010; Tian et al., 2021; Li et al., 2023).

At a global scale, crustal permeability exhibits significant stratification, influenced by both internal and external forces. In the deeper crust, internal processes such as metamorphism and magmatism are dominant, while in the shallow crust, external factors, particularly the hydrologic cycle, play a more crucial role in shaping permeability (Rojstaczer et al., 2008). The difference in permeability of the crust determines the different distribution patterns of fluids underground. Rock deformation experiments indicate that when differential stress exceeds rock shear

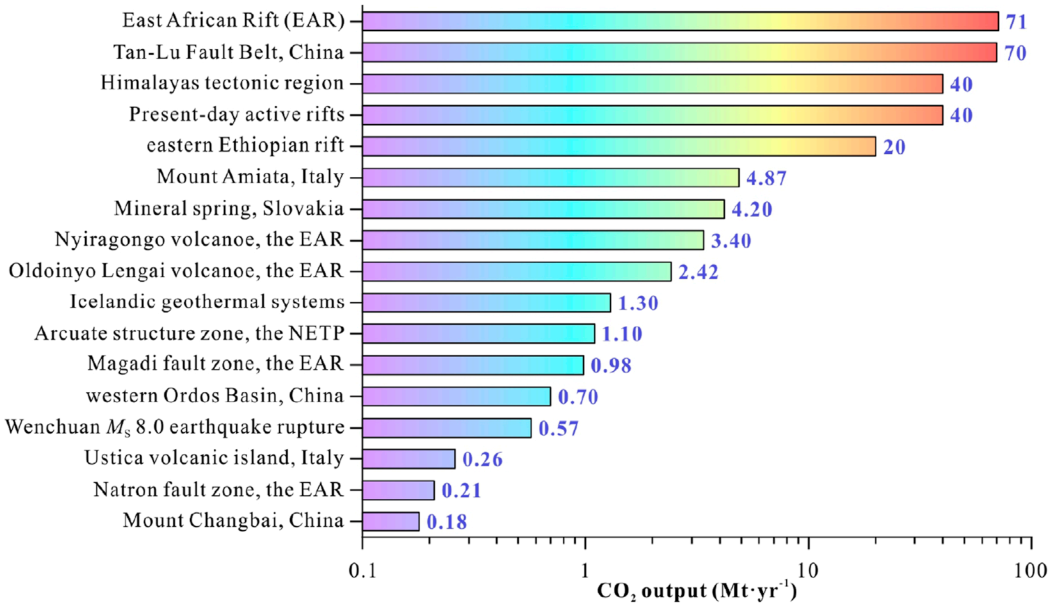

FIGURE 3
Comparison of the CO_2 output in the arcuate structure zone and other regions of the world. Data from: the East African Rift (EAR) (Lee et al., 2016); the Tan-Lu Fault Belt, China (Aulbach et al., 2020); the Himalayas tectonic region (Becker et al., 2008); the present-day active rifts (Brune et al., 2017); the eastern Ethiopian rift (Hunt et al., 2017); the Mount Amiata, Italy (Sbrana et al., 2020); the Mineral spring, Slovakia (Kučarič et al., 2015); the Nyiragongo volcanoe, the East African Rift (Sawyer et al., 2008); the Oldoinyo Lengai volcanoe, the East African Rift (Brantley and Koepenick, 1995); the Icelandic geothermal systems (Ármannsson et al., 2005); the arcuate structure zone, the northeastern Tibetan Plateau (NETP) (Liu et al., 2024); the Magadi fault zone, the East African Rift (Lee et al., 2016); the western Ordos Basin, China (Liu et al., 2023a); the Wenchuan M_S 8.0 earthquake rupture (Zhou et al., 2016); the Ustica volcanic island, Italy (Etiope et al., 1999); the Natron fault zone, the East African Rift (Lee et al., 2016); the Mount Changbai, China (Sun et al., 2021).

strength, pre-existing fractures close, forming new microcracks and pores. Continued stress can link these microcracks into macroscopic fractures, providing new pathways for fluid migration (Tuccimei et al., 2010). Under tectonic stress, the number of microcracks in fault zones increases (Li et al., 2013; Hansberry et al., 2021), accelerating the migration and release of deep gases, which can cause anomalies in gas concentrations and fluxes in shallow soils (Martinelli, 2020; Miklyaev et al., 2020). Research has shown that high sliding rates increase the permeability of sandstone and granite by three orders of magnitude, indicating that high sliding rates can sustain high permeability in fault zones (Tanikawa et al., 2010). Consequently, variations in soil gas release are primarily influenced by changes in fault zone permeability.

Active faults and fractures generally exhibit higher permeability and porosity than surrounding hard rock, resulting in greater deep-sourced gas release in fault zones compared to non-active tectonic areas (Annunziatellis et al., 2008; Giammanco et al., 2009; Weinlich, 2014; Voltattorni et al., 2015; Singh et al., 2016; Bond et al., 2017). In regions outside fault zones with lower permeability, the correlation between Rn and CO_2 concentrations is weak. In contrast, well-connected faults show a stronger positive correlation between Rn and CO_2 (Padrón et al., 2013; Ciotoli et al., 2014). Extensional structures with high permeability are more conducive to deep fluid release than thrust or strike-slip faults, with the scale of extensional faults directly influencing CO_2 emissions (Tamburello et al., 2018). For example, CO_2 emissions from the East African Rift are ~71 Mt·yr^{-1} (Lee et al., 2016), from active rifts ~40 Mt·yr^{-1} (Brune et al., 2017), and from the eastern Ethiopian Rift ~20 Mt·yr^{-1} (Hunt et al., 2017) (Figure 3). Although active faults are key pathways for the release of mantle-derived and crust-derived gases (Caracausi et al., 2022), atmospheric gases can also enter the Earth's interior through high-permeability fractures, with diffusion rates reaching 10 m·d^{-1} and maximum depths of 300 m (Arai et al., 2001; Giammanco et al., 2009). Additionally, thick sedimentary layers can obstruct gas migration, influencing atmospheric mixing and the release of deep-sourced gases, while shallow organic gases may mix with rising fluids (Liu, 2006). Therefore, the connectivity of fault zones significantly affects underground gas release, with surface gases reflecting a mix of various sources.

Deep and large active fault zones act as links across different Earth layers. Stable isotopes of deep fluids may undergo equilibrium or kinetic fractionation during geological processes, and fluid isotope tracers can provide important information on fluid sources and migration in active fault zones (Zheng et al., 2013; Zhang et al., 2021). For instance, (Hernández Perez et al., 2003) identified mantle-derived CO_2 in soil gases of the Hakkoda Fault zone in northern Japan, with a contribution of up to 6.7%. Kulongoski et al. (2013) detected high $^3He/^4He$ ratios and CO_2 concentrations in hot spring gases from the San Andreas Fault zone, with mantle-derived He contributing up to 44%. Shao et al. (2024) analyzed hot spring gases in the southern segment of the eastern boundary of the Sichuan-Yunnan rhombic block, finding no intersection between the Red River Fault and

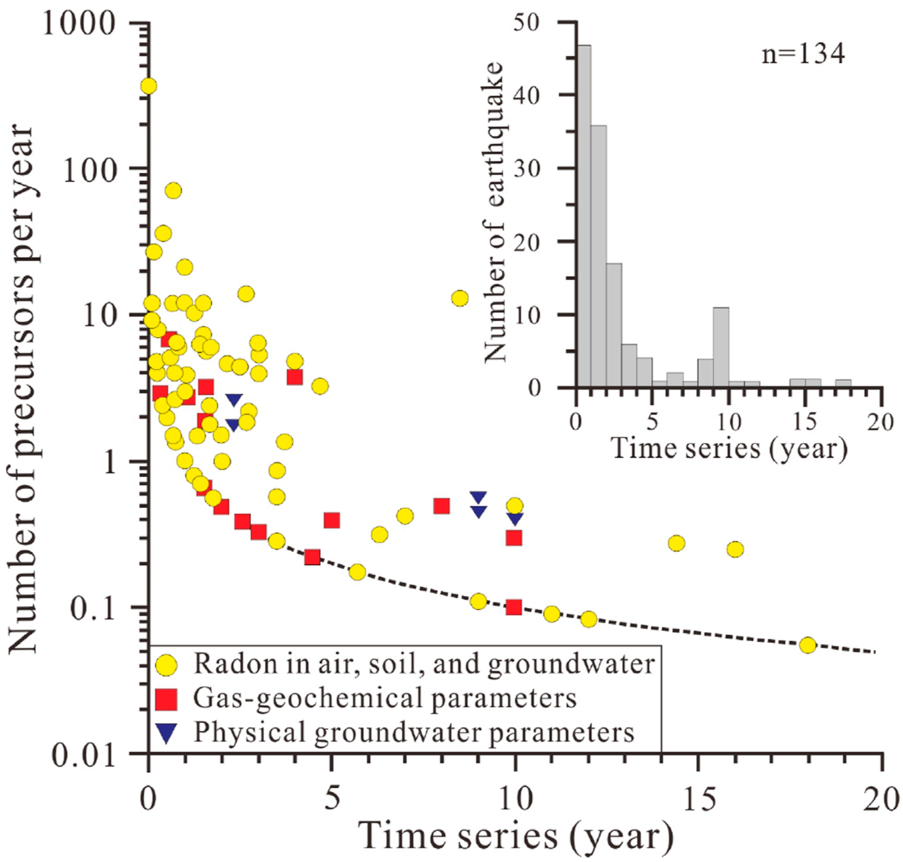

FIGURE 4
Global earthquake precursor statistics from 1967 to 2014, adapted from Woith (2015).

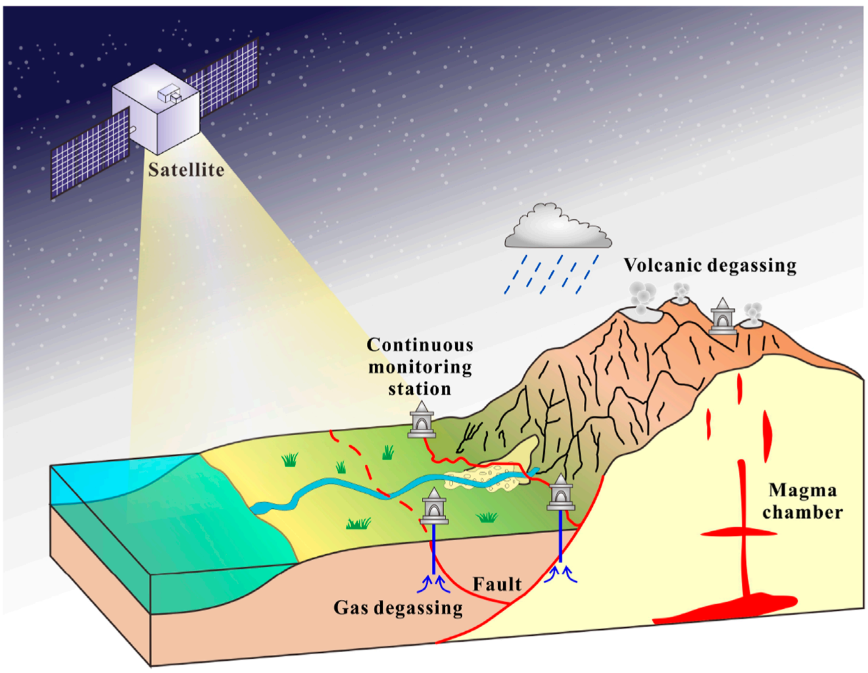

FIGURE 5
Schematic diagram of satellite hyperspectral sensors and continuous monitoring station.

Xiaojiang Fault. Zhang et al. (2021) studied the southeastern margin of the Tibetan Plateau using the He-CO_2-N_2 system in hydrothermal fluids, finding that He isotopes provided evidence for the lateral expansion and localized surface uplift of the Tibetan Plateau. These studies demonstrate that surface-emitted gases and isotopes in hot springs or soil gases are effective indicators of tectonic activity and fluid dynamics.

3.2 Relationship between fault zone gases and seismic activity

Stress changes induced by earthquakes can trigger variations in pore pressure and the number of micro-cracks within fault zones, affecting the interaction between fluids and rocks and altering the release of deep gases at the surface (Camarda et al., 2016; Randazzo et al., 2021; Zhao et al., 2021; Caracausi et al., 2022). These processes can enhance fluid migration along active faults and modify the contribution of different fluid sources to soil gases and hot spring emissions, leading to observable pre-seismic anomalies or post-seismic responses (Martinelli and Dadomo, 2017). Between 1967 and 2014, analysis of 134 global seismic cases revealed that 69% showed anomalies in soil and groundwater Rn, 20% in geochemical parameters of soil and groundwater gases, and 10% in physical groundwater parameters (Woith, 2015) (Figure 4).

Recent studies have increasingly applied geochemical methods for analyzing soil gases to understand seismic activity trends and to develop earthquake monitoring and prediction theories. In tectonically active regions, stress accumulation from seismic activity enhances the release of deep-sourced gases like Rn, CO_2, and He, which accumulate in rock fractures along fault zones (Ciotoli et al., 2014; Yuce et al., 2017; Chen et al., 2015). The correlation between Rn and CO_2 concentrations tends to increase before earthquakes (Fu et al., 2017). The vibroseis truck (Gresse et al., 2016) and active seismic source (Liu et al., 2023b) experiments have demonstrated that seismic waves can boost the release of gases trapped in rock and soil pores. Moreover, low-magnitude earthquakes ($M < 4$) can release crustal He into the atmosphere, with the He release amount being quantitatively related to the fault zone volume (Caracausi et al., 2022). Periodic monitoring of soil gases in Italy's Emilia region revealed significant increases in CO_2, CH_4, and H_2 concentrations before and after the 2012 Emilia-Romagna earthquake swarm (Sciarra et al., 2017). In Gujarat, India, continuous Rn monitoring successfully detected significant increases in Rn concentrations days to weeks before four earthquakes with magnitudes ranging from 4.0 to 4.1 (Sahoo et al., 2020; Torkar et al., 2010) used soil gas Rn to predict 10 out of 13 earthquake events using an artificial neural network with a backpropagation algorithm. These findings highlight that seismic activity induces the release of deep-sourced gases along fault zones, leading to changes in soil gas concentrations that can serve as indicators for seismic activity and earthquake monitoring.

Hot spring gas geochemistry also shows potential as an indicator of seismic activity. Before the 2008 Tibet M 6.3 earthquake in China, significant anomalies in He and Rn concentrations were observed in hot springs at Bakreswar and Tatta Pani in India (Chaudhuri et al., 2011). Prior to the 1955 Kobe M_W 6.9 earthquake in Japan, Rn release rates in groundwater and atmospheric Rn concentrations significantly increased, correlating with crustal strain fluctuations (Yasuoka et al., 2009). During the 2016 Kumamoto M 7.3 earthquake in Japan, He concentration changes in deep groundwater correlated with volumetric strain changes (Sano et al., 2016). Thus, hot spring gas concentrations can be crucial for earthquake monitoring.

Throughout different stages of earthquake preparation and occurrence, the contribution of deep-sourced and shallow-sourced fluids dynamically evolves. For instance, before and after the 2011 Van M_W 7.2 earthquake in Turkey (Aydın et al., 2015) and the 2013 Lushan M_S 7.0 earthquake in China (Chen et al., 2015), significant increases in $^3He/^4He$ and $\delta^{13}C_{CO2}$ values were observed in hot spring gases in fault zones. As aftershock activity waned, the supply of mantle-derived gases decreased, leading to a decline in $^3He/^4He$ and $\delta^{13}C_{CO2}$ values. Following the 2008 Iwate-Miyagi M 7.2 earthquake in Japan, the ascent of mantle-derived fluids caused a maximum 85% increase in the $^3He/^4He$ value in hot spring gases near the epicenter within a week (Horiguchi and Matsuda, 2008). After 2 M 6.0 earthquakes in the Emilia, Italy in 2012, the $\delta^{13}C_{CO2}$ and $\delta^{13}C_{CH4}$ values of gases released from fault zones in the epicentral area significantly decreased, likely due to the seismic-induced release of shallow biogenic CH_4 and CO_2, overshadowing deep thermogenic gases (Sciarra et al., 2017). These changes in He and C isotopes in hot spring gases near fault zones before and after earthquakes underscore how seismic activity promotes the mixing of gases from various sources, particularly the ascent of mantle-derived fluids.

Atmospheric gas variations induced by seismic activity are integral to understanding the lithosphere-atmosphere coupling mechanism (Veefkind et al., 2012; Jing et al., 2019). Advances in hyperspectral sensors with atmospheric detection capabilities have enabled extensive studies on gas changes associated with seismic and volcanic events (Tramutoli et al., 2013) (Figure 5). Notable anomalies in gases such as CH_4, CO, CO_2 and O_3 have been documented before and after significant earthquakes, such as the 2004 Sumatra-Andaman M_W 9.1 earthquake and the 2005 Sumatra-Nias M_W 8.6 earthquake (Cui et al., 2023), the 2008 Wenchuan M_S 8.0 earthquake and 2013 Lushan M_S 7.0 earthquake in China (Cui et al., 2017), and the 2015 Gorkha M 7.8 earthquake and Dolakha M 7.3 earthquake in Nepal (Jing et al., 2019). Furthermore, a statistical analysis using the Adaboost machine learning algorithm examined infrared and hyperspectral gas parameters among 10 different variables before and after 1,371 global earthquakes of magnitude ≥6 from 2006 to 2013, identifying O_3 and CO_2 as significant contributors to earthquake prediction (Xiong et al., 2021).

4 Conclusion

Active fault zones are vital conduits for deep fluids migrating to the Earth's surface. The gases released (such as CO_2, Rn, and He) contain valuable information about the physical and chemical evolution of the Earth's interior and further reveal fault activity and seismic events. Isotope tracing is essential for identifying fluid sources, migration pathways, circulation processes, and formation mechanisms.

Gas release in fault zones is closely related to fault activity, and higher fault activity corresponds to higher soil gas release. Different fault types exhibit distinct geochemical fluid characteristics. Fault zones with strong gas release are preferred locations for studying regional geodynamics and monitoring subsurface tectonic activities.

Seismic activity alters stress states, which promotes the release of deep-sourced gases along fault zones and leads to anomalies in concentrations of soil gas and hot spring gas. These anomalies can serve as indicators of seismic activity, providing crucial information for earthquake monitoring. Isotopic changes in hot spring gases before and after earthquakes further demonstrate that seismic activity promotes the mixing of gases from different sources, especially the ascent of crustal or mantle-derived fluids.

In summary, fault zones are crucial for deep fluid migration and as research subjects for monitoring tectonic activity and earthquake prediction. Analyzing fault zone gas geochemistry enhances our understanding of the material cycle and energy exchange processes in the Earth's interior, providing a scientific basis for disaster prevention and mitigation.

Author contributions

JL: Conceptualization, Data curation, Formal Analysis, Funding acquisition, Investigation, Methodology, Project administration, Resources, Software, Supervision, Validation, Visualization, Writing–original draft, Writing–review and editing. ZL: Conceptualization, Data curation, Formal Analysis, Funding acquisition, Investigation, Methodology, Project administration, Resources, Software, Supervision, Validation, Visualization, Writing–original draft, Writing–review and editing. ZC: Writing–original draft, Writing–review and editing. YG: Conceptualization, Data curation, Formal Analysis, Writing–original draft. YH: Conceptualization, Data curation, Formal Analysis, Writing–original draft. HG: Conceptualization, Data curation, Formal Analysis, Funding acquisition, Writing–original draft.

Funding

The author(s) declare that financial support was received for the research, authorship, and/or publication of this article. This work was supported by the National Natural Science Foundation of China (Grant No. 42372282) and the Science for Earthquake Resilience of China Earthquake Administration (Grant No. XH22035).

Conflict of interest

The authors declare that the research was conducted in the absence of any commercial or financial relationships that could be construed as a potential conflict of interest.

Publisher's note

All claims expressed in this article are solely those of the authors and do not necessarily represent those of their affiliated organizations, or those of the publisher, the editors and the reviewers. Any product that may be evaluated in this article, or claim that may be made by its manufacturer, is not guaranteed or endorsed by the publisher.

References

Andrews, J. N. (1985). The isotopic composition of radiogenic helium and its use to study groundwater movement in confined aquifers. *Chem. Geol.* 49 (1), 339–351. doi:10.1016/0009-2541(85)90166-4

Annunziatellis, A., Beaubien, S., Bigi, S., Ciotoli, G., Coltella, M., and Lombardi, S. (2008). Gas migration along fault systems and through the vadose zone in the Latera caldera (central Italy): implications for CO_2 geological storage. *Int. J. Greenh. Gas. Control.* 2 (3), 353–372. doi:10.1016/j.ijggc.2008.02.003

Arai, T., Okusawa, T., and Tsukahara, H. (2001). Behavior of gases in the Nojima Fault Zone revealed from the chemical composition and carbon isotope ratio of gases extracted from DPRI 1800 m drill core. *Isl. Arc.* 10 (3-4), 430–438. doi:10.1111/j.1440-1738.2001.00341.x

Ármannsson, H., Fridriksson, T., and Kristjánsson, B. R. (2005). CO_2 emissions from geothermal power plants and natural geothermal activity in Iceland. *Geothermics* 34 (3), 286–296. doi:10.1016/j.geothermics.2004.11.005

Audi, G., Bersillon, O., Blachot, J., and Wapstra, A. H. (2003). The Nubase evaluation of nuclear and decay properties. *Nucl. Phys. A* 729 (1), 3–128. doi:10.1016/j.nuclphysa.2003.11.001

Aulbach, S., Lin, A. B., Weiss, Y., and Yaxley, G. M. (2020). Wehrlites from continental mantle monitor the passage and degassing of carbonated melts. *Geochem. Perspect. Lett.* 15, 30–34. doi:10.7185/geochemlet.2031

Aydın, H., Hilton, D. R., Güleç, N., and Mutlu, H. (2015). Post-earthquake anomalies in He-CO_2 isotope and relative abundance systematics of thermal waters: the case of the 2011 Van earthquake, eastern Anatolia, Turkey. *Chem. Geol.* 411, 1–11. doi:10.1016/j.chemgeo.2015.06.019

Barnes, I., Irwin, W. P., and White, D. E. (1978). *Global distribution of carbon dioxide discharges, and major zones of seismicity*. Menlo Park: United States: United States Department of the Interior Geological Survey.

Becker, J. A., Bickle, M. J., Galy, A., and Holland, T. J. B. (2008). Himalayan metamorphic CO_2 fluxes: Quantitative constraints from hydrothermal springs. *Earth Planet. Sci. Lett.* 265 (3), 616–629. doi:10.1016/j.epsl.2007.10.046

Bergfeld, D., Goff, F., and Janik, C. J. (2001). Carbon isotope systematics and CO_2 sources in the Geysers-Clear Lake region, northern California, USA. *Geothermics* 30 (2-3), 303–331. doi:10.1016/S0375-6505(00)00051-1

Bhongsuwan, T., Pisapak, P., and Dürrast, H. (2011). Result of alpha track detection of radon in soil gas in the Khlong Marui Fault Zone, Southern Thailand: a possible earthquake precursor. *Wārasān Songkhlā Nakharin* 33 (5), 609–616.

Bond, C. E., Kremer, Y., Johnson, G., Hicks, N., Lister, R., Jones, D. G., et al. (2017). The physical characteristics of a CO_2 seeping fault: the implications of fracture permeability for carbon capture and storage integrity. *Int. J. Greenh. Gas. Control.* 61, 49–60. doi:10.1016/j.ijggc.2017.01.015

Brantley, S. L., and Koepenick, K. W. (1995). Measured carbon dioxide emissions from Oldoinyo Lengai and the skewed distribution of passive volcanic fluxes. *Geology* 23 (10), 933–936. doi:10.1130/0091-7613(1995)023<0933:mcdefo>2.3.co;2

Brune, S., Williams, S. E., and Müller, R. D. (2017). Potential links between continental rifting, CO_2 degassing and climate change through time. *Nat. Geosci.* 10 (12), 941–946. doi:10.1038/s41561-017-0003-6

Camarda, M., De Gregorio, S., Di Martino, R. M. R., and Favara, R. (2016). Temporal and spatial correlations between soil CO_2 flux and crustal stress. *J. Geophys. Res. Solid Earth.* 121 (10), 7071–7085. doi:10.1002/2016JB013297

Capaccioni, B., Tassi, F., Cremonini, S., Sciarra, A., and Vaselli, O. (2015). Ground heating and methane oxidation processes at shallow depth in Terre Calde di Medolla (Italy): Observations and conceptual model. *J. Geophys. Res. Solid Earth.* 120 (5), 3048–3064. doi:10.1002/2014JB011635

Caracausi, A., Buttitta, D., Picozzi, M., Paternoster, M., and Stabile, T. A. (2022). Earthquakes control the impulsive nature of crustal helium degassing to the atmosphere. *Commun. Earth Environ.* 3 (1), 224. doi:10.1038/s43247-022-00549-9

Chaudhuri, H., Bari, W., Iqbal, N., Bhandari, R. K., Ghose, D., Sen, P., et al. (2011). Long range gas-geochemical anomalies of a remote earthquake recorded simultaneously at distant monitoring stations in India. *Geochem. J.* 45 (2), 137–156. doi:10.2343/geochemj.1.0109

Chen, Z., Li, Y., Liu, Z., Wang, J., Zhou, X., and Du, J. (2018). Radon emission from soil gases in the active fault zones in the Capital of China and its environmental effects. *Sci. Rep.* 8 (1), 16772. doi:10.1038/s41598-018-35262-1

Chen, Z., Zhou, X., Du, J., Xie, C., Liu, L., Li, Y., et al. (2015). Hydrochemical characteristics of hot spring waters in the Kangding district related to the Lushan M_S=7.0 earthquake in Sichuan, China. *Nat. Hazards Earth Syst. Sci.* 15 (6), 1149–1156. doi:10.5194/nhess-15-1149-2015

Cheng, Y., Wang, N., and Hou, S. (2005). *Nuclear radiation field and radioactive exploration*. Beijing: Geology Press. (in Chinese).

Ciotoli, G., Bigi, S., Tartarello, C., Sacco, P., Lombardi, S., Ascione, A., et al. (2014). Soil gas distribution in the main coseismic surface rupture zone of the 1980, M_S=6.9, Irpinia earthquake (southern Italy). *J. Geophys. Res. Solid Earth.* 119 (3), 2440–2461. doi:10.1002/2013JB010508

Ciotoli, G., Lombardi, S., and Annunziatellis, A. (2007). Geostatistical analysis of soil gas data in a high seismic intermontane basin: Fucino Plain, central Italy. *J. Geophys. Res. Solid Earth.* 112 (B5), B05407. doi:10.1029/2005JB004044

Cui, Y., Ouzounov, D., Hatzopoulos, N., Sun, K., Zou, Z., and Du, J. (2017). Satellite observation of CH4 and CO anomalies associated with the Wenchuan M_S 8.0 and Lushan M_S 7.0 earthquakes in China. *Chem. Geol.* 469, 185–191. doi:10.1016/j.chemgeo.2017.06.028

Cui, Y., Zheng, C., Jiang, L., Huang, J., Sun, F., Zou, Z., et al. (2023). Variations of multiple gaseous emissions associated with the great Sumatra earthquakes in 2004 and 2005. *Chem. Geol.* 618, 121311. doi:10.1016/j.chemgeo.2023.121311

Di Martino, R. M. R., Capasso, G., and Camarda, M. (2016). Spatial domain analysis of carbon dioxide from soils on Vulcano Island: implications for CO_2 output evaluation. *Chem. Geol.* 444, 59–70. doi:10.1016/j.chemgeo.2016.09.037

El-Arabi, A. M., Abbady, A., Ahmed, N. K., Michel, R., El-Kamel, A. H., and Abbady, A. G. E. (2006). Assessment of radon-222 concentrations and exhalation rates of rocks and building materials. *Indian J. Pure Appl. Phys.* 44 (4), 287–291.

Etiope, G., Beneduce, P., Calcara, M., Favali, P., Frugoni, F., Schiattarella, M., et al. (1999). Structural pattern and CO_2-CH_4 degassing of Ustica island, southern Tyrrhenian basin. *J. Volcanol. Geotherm. Res.* 88 (4), 291–304. doi:10.1016/S0377-0273(99)00010-4

Etiope, G., and Martinelli, G. (2002). Migration of carrier and trace gases in the geosphere: an overview. *Phys. Earth Planet. Inter.* 129 (3), 185–204. doi:10.1016/S0031-9201(01)00292-8

Faulkner, D. R., Jackson, C. A. L., Lunn, R. J., Schlische, R. W., Shipton, Z. K., Wibberley, C. A. J., et al. (2010). A review of recent developments concerning the structure, mechanics and fluid flow properties of fault zones. *J. Struct. Geol.* 32 (11), 1557–1575. doi:10.1016/j.jsg.2010.06.009

Flügge, S., and Zimens, K. E. (1939). Die Bestimmung von Korngrößen und von Diffusionskonstanten aus dem Emaniervermögen. *Z. für Phys. Chem.* 42B, 179–220. doi:10.1515/zpch-1939-4215

Fu, C. C., Yang, T. F., Tsai, M. C., Lee, L. C., Liu, T. K., Walia, V., et al. (2017). Exploring the relationship between soil degassing and seismic activity by continuous radon monitoring in the Longitudinal Valley of eastern Taiwan. *Chem. Geol.* 469, 163–175. doi:10.1016/j.chemgeo.2016.12.042

Gao, Z., Chen, Z., He, H., Liu, Z., Lu, C., Wang, H., et al. (2024). Characteristics and main controlling factors of helium resources in the main petroliferous basins of the North China Craton. *Acta Oceanol. Sin.* 43 (2), 23–33. doi:10.1007/s13131-024-2290-2

Giammanco, S., Immè, G., Mangano, G., Morelli, D., and Neri, M. (2009). Comparison between different methodologies for detecting radon in soil along an active fault: the case of the Pernicana fault system, Mt. Etna (Italy). *Appl. Radiat. Isot.* 67 (1), 178–185. doi:10.1016/j.apradiso.2008.09.007

Girault, F., and Perrier, F. (2014). The Syabru-Bensi hydrothermal system in central Nepal: 2. Modeling and significance of the radon signature. *J. Geophys. Res. Solid Earth.* 119 (5), 4056–4089. doi:10.1002/2013JB010302

Graham, D. W. (2002). Noble gas isotope geochemistry of Mid-Ocean Ridge and ocean island basalts: Characterization of mantle source reservoirs. *Rev. Mineralogy Geochem.* 47 (1), 247–317. doi:10.2138/rmg.2002.47.8

Gresse, M., Vandemeulebrouck, J., Byrdina, S., Chiodini, G., and Bruno, P. P. (2016). Changes in CO_2 diffuse degassing induced by the passing of seismic waves. *J. Volcanol. Geotherm. Res.* 320, 12–18. doi:10.1016/j.jvolgeores.2016.04.019

Hansberry, R. L., King, R. C., Holford, S. P., Hand, M., and Debenham, N. (2021). How wide is a fault damage zone? Using network topology to examine how fault-damage zones overprint regional fracture networks. *J. Struct. Geol.* 146, 104327. doi:10.1016/j.jsg.2021.104327

Hernández Perez, P., Notsu, K., Tsurumi, M., Mori, T., Ohno, M., Shimoike, Y., et al. (2003). Carbon dioxide emissions from soils at Hakkoda, north Japan. *J. Geophys. Res. Solid Earth.* 108 (B4), 1–10. doi:10.1029/2002JB001847

Hong, W., Yang, T. F., Walia, V., Lin, S., Fu, C., Chen, Y., et al. (2010). Nitrogen as the carrier gas for helium emission along an active fault in NW Taiwan. *Appl. Geochem.* 25 (4), 593–601. doi:10.1016/j.apgeochem.2010.01.016

Horiguchi, K., and Matsuda, J. I. (2008). On the change of $^3He/^4He$ ratios in hot spring gases after the Iwate-Miyagi Nairiku Earthquake in 2008. *Geochem. J.* 42, e1–e4. doi:10.2343/geochemj.42.e1

Horton, F., Asimow, P. D., Farley, K. A., Curtice, J., Kurz, M. D., Blusztajn, J., et al. (2023). Highest terrestrial $^3He/^4He$ credibly from the core. *Nature* 623 (7985), 90–94. doi:10.1038/s41586-023-06590-8

Hunt, J. A., Zafu, A., Mather, T. A., Pyle, D. M., and Barry, P. H. (2017). Spatially variable CO_2 degassing in the main Ethiopian Rift: implications for magma storage, volatile transport, and rift-related emissions. *Geochem. Geophys. Geosyst.* 18 (10), 3714–3737. doi:10.1002/2017GC006975

Jaishi, H. P., Singh, S., Tiwari, R. P., and Tiwari, R. C. (2014). Correlation of radon anomalies with seismic events along Mat fault in Serchhip District, Mizoram, India. *Appl. Radiat. Isot.* 86, 79–84. doi:10.1016/j.apradiso.2013.12.040

Jing, F., Singh, R. P., and Shen, X. (2019). Land – atmosphere – Meteorological coupling associated with the 2015 Gorkha (M 7.8) and Dolakha (M 7.3) Nepal earthquakes. *Geomatics, Nat. Hazards Risk* 10 (1), 1267–1284. doi:10.1080/19475705.2019.1573629

Keeling, C. D., Piper, S. C., Bacastow, R. B., Wahlen, M., Whorf, T. P., Heimann, M., et al. (2005). *Atmospheric CO_2 and $^{13}CO_2$ exchange with the terrestrial biosphere and oceans from 1978 to 2000: observations and carbon cycle implications A History of Atmospheric CO_2 and its Effects on Plants, Animals, and Ecosystems*, 5. New York, United States: Springer New York, 83–113. (Reprinted. doi:10.1007/0-387-27048-5_5

King, C. (1978). Radon emanation on san Andreas Fault. *Nature* 271 (5645), 516–519. doi:10.1038/271516a0

Klusman, R. W. (1993). *Soil gas and related methods for natural resource exploration*. New York, United States: Wiley and Sons.

Kucharič, L. U., Bodiš, D., Panák, D., Liščák, P., and Božíková, J. (2015). A contribution of CO_2 released from mineral springs into overall volume of annual CO_2 emissions in the Slovak Republic. *Environ. Earth Sci.* 73 (1), 231–238. doi:10.1007/s12665-014-3418-z

Kulongoski, J. T., Hilton, D. R., Barry, P. H., Esser, B. K., Hillegonds, D., and Belitz, K. (2013). Volatile fluxes through the Big Bend section of the san Andreas Fault, California: helium and carbon-dioxide systematics. *Chem. Geol.* 339, 92–102. doi:10.1016/j.chemgeo.2012.09.007

Lee, H., Kim, H., Kagoshima, T., Park, J., Takahata, N., and Sano, Y. (2019). Mantle degassing along strike-slip faults in the Southeastern Korean Peninsula. *Sci. Rep.* 9 (1), 15334. doi:10.1038/s41598-019-51719-3

Lee, H., Muirhead, J. D., Fischer, T. P., Ebinger, C. J., Kattenhorn, S. A., Sharp, Z. D., et al. (2016). Massive and prolonged deep carbon emissions associated with continental rifting. *Nat. Geosci.* 9 (2), 145–149. doi:10.1038/ngeo2622

Li, Y., Chen, Z., Sun, A., Liu, Z., Caracausi, A., Martinelli, G., et al. (2023). Geochemical features and seismic imaging of the tectonic zone between the Tibetan Plateau and Ordos Block, central northern China. *Chem. Geol.* 622, 121386. doi:10.1016/j.chemgeo.2023.121386

Li, Y., Du, J., Wang, X., Zhou, X., Xie, C., and Cui, Y. (2013). Spatial variations of soil gas geochemistry in the Tangshan area of northern China. *Terr. Atmos. Ocean. Sci.* 24 (3), 323–332. doi:10.3319/TAO.2012.11.26.01(TT

Liu, J. H. (2006). *Numerical simulation, inversion fitting of radon migration in the overburden above active fault*. China: Jilin University, 1–155. (in Chinese with English abstract).

Liu, L., Chen, Z., Li, Y., Liu, Z., Hu, L., Wang, X., et al. (2023b). Emission of Rn and CO_2 from soil at fault zones caused by seismic waves. *Earth Space Sci.* 10 (6), e2023EA003012. doi:10.1029/2023EA003012

Liu, Z., Chen, Z., Li, Y., Zhao, Z., Sun, A., Li, J., et al. (2024). Crust uplift controls the massive emissions of 222Rn and CO_2 in the Northeastern Tibetan Plateau, China. *Chem. Geol.* 663, 122280. doi:10.1016/j.chemgeo.2024.122280

Liu, Z., Li, Y., Chen, Z., Zhao, Z., Huangfu, R., Zhao, Y., et al. (2023a). Environmental impacts of ^{222}Rn, Hg and CO_2 emissions from the fault zones in the western margin of the Ordos block, China. *Environ. Geochem. Health.* 45 (2), 457–472. doi:10.1007/s10653-022-01350-5

Lupton, J. E. (1983). Terrestrial inert gases; Isotope tracer studies and clues to primordial components in the mantle. *Annu. Rev. Earth Planet. Sci.* 11 (1), 371–414. doi:10.1146/annurev.ea.11.050183.002103

Manisa, K., Erdogan, M., Zedef, V., Bircan, H., and Biçer, A. (2022). Variations of ^{222}Rn concentrations over active fault system in Simav, Kütahya, Western Turkey:

possible causes for soil-gas 222Rn anomalies. *Appl. Radiat. Isot.* 190, 110484. doi:10.1016/j.apradiso.2022.110484

Martinelli, G. (2020). Previous, current, and future trends in research into earthquake precursors in geofluids. *Geosciences* 10 (5), 189. doi:10.3390/geosciences10050189

Martinelli, G., Albarello, D., and Mucciarelli, M. (1995). Radon emissions from mud volcanoes in northern Italy; Possible connection with local seismicity. *Geophys. Res. Lett.* 22 (15), 1989–1992. doi:10.1029/95GL01785

Martinelli, G., and Dadomo, A. (2017). Factors constraining the geographic distribution of earthquake geochemical and fluid-related precursors. *Chem. Geol.* 469, 176–184. doi:10.1016/j.chemgeo.2017.01.006

Miklyaev, P. S., Petrova, T. B., Marennyy, A. M., Shchitov, D. V., Sidyakin, P. A., Murzabekov, M., et al. (2020). High seasonal variations of the radon exhalation from soil surface in the fault zones (Baikal and North Caucasus regions). *J. Environ. Radioact.* 219, 106271. doi:10.1016/j.jenvrad.2020.106271

Muto, J., Yasuoka, Y., Miura, N., Iwata, D., Nagahama, H., Hirano, M., et al. (2021). Preseismic atmospheric radon anomaly associated with 2018 Northern Osaka earthquake. *Sci. Rep.* 11 (1), 7451. doi:10.1038/s41598-021-86777-z

Padrón, E., Padilla, G., Hernández, P. A., Pérez, N. M., Calvo, D., Nolasco, D., et al. (2013). Soil gas geochemistry in relation to eruptive fissures on Timanfaya volcano, Lanzarote Island (Canary Islands, Spain). *J. Volcanol. Geotherm. Res.* 250, 91–99. doi:10.1016/j.jvolgeores.2012.10.013

Pankina G, R., Mekhtieva, L. V., Gurieva, M. S., and Shkutnik, N. E. (1979). Origin of CO_2 in petroleum gases (from the isotopic composition of carbon). *Int. Geol. Rev.* 21 (5), 535–539. doi:10.1080/00206818209467089

Papastefanou, C. (2010). Variation of radon flux along active fault zones in association with earthquake occurrence. *Radiat. Meas.* 45 (8), 943–951. doi:10.1016/j.radmeas.2010.04.015

Parks, M. M., Caliro, S., Chiodini, G., Pyle, D. M., Mather, T. A., Berlo, K., et al. (2013). Distinguishing contributions to diffuse CO_2 emissions in volcanic areas from magmatic degassing and thermal decarbonation using soil gas ^{222}Rn-$\delta^{13}C$ systematics: Application to Santorini volcano, Greece. *Earth Planet. Sci. Lett.* 377-378, 180–190. doi:10.1016/j.epsl.2013.06.046

Pereira, A., Lamas, R., Miranda, M., Domingos, F., Neves, L., Ferreira, N., et al. (2017). Estimation of the radon production rate in granite rocks and evaluation of the implications for geogenic radon potential maps: a case study in Central Portugal. *J. Environ. Radioact.* 166, 270–277. doi:10.1016/j.jenvrad.2016.08.022

Phong Thu, H. N., Van Thang, N., and Hao, L. C. (2020). The effects of some soil characteristics on radon emanation and diffusion. *J. Environ. Radioact.* 216, 106189. doi:10.1016/j.jenvrad.2020.106189

Porstendörfer, J. (1994). Properties and behaviour of radon and thoron and their decay products in the air. *J. Aerosol Sci.* 25 (2), 219–263. doi:10.1016/0021-8502(94)90077-9

Randazzo, P., Caracausi, A., Aiuppa, A., Cardellini, C., Chiodini, G., D'Alessandro, W., et al. (2021). Active degassing of deeply sourced fluids in Central Europe: new evidences from a geochemical study in Serbia. *Geochem. Geophys. Geosyst.* 22 (11), e2021GC010017. doi:10.1029/2021GC010017

Rojstaczer, S. A., Ingebritsen, S. E., and Hayba, D. O. (2008). Permeability of continental crust influenced by internal and external forcing. *Geofluids* 8 (2), 128–139. doi:10.1111/j.1468-8123.2008.00211.x

Rovira, P., and Vallejo, V. R. (2008). Changes in $\delta^{13}C$ composition of soil carbonates driven by organic matter decomposition in a Mediterranean climate: a field incubation experiment. *Geoderma* 144 (3), 517–534. doi:10.1016/j.geoderma.2008.01.006

Sahoo, S. K., Katlamudi, M., Barman, C., and Lakshmi, G. U. (2020). Identification of earthquake precursors in soil radon-222 data of Kutch, Gujarat, India using empirical mode decomposition based Hilbert Huang Transform. *J. Environ. Radioact.* 222, 106353. doi:10.1016/j.jenvrad.2020.106353

Sakoda, A., Ishimori, Y., and Yamaoka, K. (2011). A comprehensive review of radon emanation measurements for mineral, rock, soil, mill tailing and fly ash. *Appl. Radiat. Isot.* 69 (10), 1422–1435. doi:10.1016/j.apradiso.2011.06.009

Sano, Y., Takahata, N., Kagoshima, T., Shibata, T., Onoue, T., and Zhao, D. (2016). Groundwater helium anomaly reflects strain change during the 2016 Kumamoto earthquake in Southwest Japan. *Sci. Rep.* 6, 37939. doi:10.1038/srep37939

Sano, Y., and Wakita, H. (1985). Geographical distribution of $^3He/^4He$ ratios in Japan: implications for arc tectonics and incipient magmatism. *J. Geophys. Res. Solid Earth.* 90 (B10), 8729–8741. doi:10.1029/JB090iB10p08729

Sawyer, G. M., Carn, S. A., Tsanev, V. I., Oppenheimer, C., and Burton, M. (2008). Investigation into magma degassing at Nyiragongo volcano, Democratic Republic of the Congo. *Geochem. Geophys. Geosyst.* 9 (2), Q02017. doi:10.1029/2007GC001829

Sbrana, A., Marianelli, P., Belgiorno, M., Sbrana, M., and Ciani, V. (2020). Natural CO_2 degassing in the Mount Amiata volcanic-geothermal area. *J. Volcanol. Geotherm. Res.* 397, 106852. doi:10.1016/j.jvolgeores.2020.106852

Sciarra, A., Cantucci, B., and Coltorti, M. (2017). Learning from soil gas change and isotopic signatures during 2012 Emilia seismic sequence. *Sci. Rep.* 7 (1), 14187. doi:10.1038/s41598-017-14500-y

Seminsky, K. Z., Demberel, S., Tugarina, M. A., Ganzorig, D., and Bornyakov, S. A. (2013). First estimates of soil radon activity in the fault zones of central Mongolia. *Dokl. Earth Sci.* 448 (1), 21–24. doi:10.1134/S1028334X12110128

Shao, W., Liu, Z., Li, Y., Chen, Z., Lu, C., Zhao, C., et al. (2024). Geochemical characteristics of thermal springs and insights into the intersection between the Xiaojiang Fault and the red River Fault, southeastern Tibet plateau. *Geochem. Geophys. Geosyst.* 25 (3), e2023GC011431. doi:10.1029/2023GC011431

Singh, S., Jaishi, H. P., Tiwari, R. P., and Tiwari, R. C. (2016). A study of variation in soil gas concentration associated with earthquakes near Indo-Burma Subduction zone. *Geoenviron. Disasters* 3 (22), 22–28. doi:10.1186/s40677-016-0055-8

Soddy, F. (1913). "Radioactivity," in *Annual Reports on the Progress of Chemistry* (London: The Chemical Society), 262–288.

Sun, X., Yang, P., Xiang, Y., Si, X., and Liu, D. (2018). Across-fault distributions of radon concentrations in soil gas for different tectonic environments. *Geosci. J.* 22 (2), 227–239. doi:10.1007/s12303-017-0028-2

Sun, Y., Guo, Z., and Fortin, D. (2021). Carbon dioxide emission from monogenetic volcanoes in the Mt. Changbai volcanic field, NE China. *Int. Geol. Rev.* 63 (13-14), 1803–1820. doi:10.1080/00206814.2020.1802782

Tamburello, G., Pondrelli, S., Chiodini, G., and Rouwet, D. (2018). Global-scale control of extensional tectonics on CO_2 earth degassing. *Nat. Commun.* 9 (1), 4608. doi:10.1038/s41467-018-07087-z

Tamir, G., Shenker, M., Heller, H., Bloom, P. R., Fine, P., and Bar-Tal, A. (2011). Can soil carbonate dissolution lead to overestimation of soil respiration? *Soil Sci. Soc. Am. J.* 75 (4), 1414–1422. doi:10.2136/sssaj2010.0396

Tan, C. (2016). Big gaps and short bridges: a model for solving the discontinuity problem. *Answers Res. J.* 9, 149–162.

Tanikawa, W., Sakaguchi, M., Tadai, O., and Hirose, T. (2010). Influence of fault slip rate on shear-induced permeability. *J. Geophys. Res. Solid Earth.* 115 (B07412), 1–18. doi:10.1029/2009JB007013

Tian, J., Pang, Z., Liao, D., and Zhou, X. (2021). Fluid geochemistry and its implications on the role of deep faults in the genesis of high temperature systems in the eastern edge of the Qinghai Tibet Plateau. *Appl. Geochem.* 131, 105036. doi:10.1016/j.apgeochem.2021.105036

Torkar, D., Zmazek, B., Vaupotič, J., and Kobal, I. (2010). Application of artificial neural networks in simulating radon levels in soil gas. *Chem. Geol.* 270, 1–8. doi:10.1016/j.chemgeo.2009.09.017

Tramutoli, V., Aliano, C., Corrado, R., Filizzola, C., Genzano, N., Lisi, M., et al. (2013). On the possible origin of thermal infrared radiation (TIR) anomalies in earthquake-prone areas observed using robust satellite techniques (RST). *Chem. Geol.* 339, 157–168. doi:10.1016/j.chemgeo.2012.10.042

Tuccimei, P., Mollo, S., Vinciguerra, S., Castelluccio, M., and Soligo, M. (2010). Radon and thoron emission from lithophysae-rich tuff under increasing deformation: an experimental study. *Geophys. Res. Lett.* 37 (L05305), 1–5. doi:10.1029/2009GL042134

Veefkind, J. P., Aben, I., McMullan, K., Förster, H., de Vries, J., Otter, G., et al. (2012). TROPOMI on the ESA Sentinel-5 Precursor: a GMES mission for global observations of the atmospheric composition for climate, air quality and ozone layer applications. *Remote Sens. Environ.* 120, 70–83. doi:10.1016/j.rse.2011.09.027

Voltattorni, N., Lombardi, S., and Beaubien, S. E. (2015). Gas migration from two mine districts: the Tolfa (Lazio, Central Italy) and the Neves-Corvo (Baixo Alentejo, Portugal) case studies. *J. Geochem. Explor.* 152, 37–53. doi:10.1016/j.gexplo.2015.01.011

Walia, V., Lin, S. J., Fu, C. C., Yang, T. F., Hong, W., Wen, K., et al. (2010). Soil-gas monitoring: a tool for fault delineation studies along Hsinhua fault (Tainan), southern Taiwan. *Appl. Geochem.* 25 (4), 602–607. doi:10.1016/j.apgeochem.2010.01.017

Weinlich, F. H. (2014). Carbon dioxide controlled earthquake distribution pattern in the NW Bohemian swarm earthquake region, western Eger Rift, Czech Republic - gas migration in the crystalline basement. *Geofluids* 14 (2), 143–159. doi:10.1111/gfl.12058

White, D. E. (1957). Magmatic, connate and metamorphic waters. *Geol. Soc. Am. Bull.* 68 (12), 1659–1682. doi:10.1130/0016-7606(1957)68[1659:mcamw]2.0.co;2

Woith, H. (2015). Radon earthquake precursor: a short review. *Eur. Phys. J. ST, Special Top.* 224 (4), 611–627. doi:10.1140/epjst/e2015-02395-9

Xiong, P., Tong, L., Zhang, K., Shen, X., Battiston, R., Ouzounov, D., et al. (2021). Towards advancing the earthquake forecasting by machine learning of satellite data. *Sci. Total Environ.* 771, 145256. doi:10.1016/j.scitotenv.2021.145256

Yasuoka, Y., Kawada, Y., Nagahama, H., Omori, Y., Ishikawa, T., Tokonami, S., et al. (2009). Preseismic changes in atmospheric radon concentration and crustal strain. *Phys. Chem. Earth.* 34 (6-7), 431–434. doi:10.1016/j.pce.2008.06.005

Yuce, G., Fu, C. C., D'Alessandro, W., Gulbay, A. H., Lai, C. W., Bellomo, S., et al. (2017). Geochemical characteristics of soil radon and carbon dioxide within the Dead Sea Fault and Karasu Fault in the Amik basin (Hatay), Turkey. *Chem. Geol.* 469, 129–146. doi:10.1016/j.chemgeo.2017.01.003

Zhang, M., Guo, Z., Xu, S., Barry, P. H., Sano, Y., Zhang, L., et al. (2021). Linking deeply-sourced volatile emissions to plateau growth dynamics in southeastern Tibetan Plateau. *Nat. Commun.* 12 (1), 4157. doi:10.1038/s41467-021-24415-y

Zhao, Y., Liu, Z., Li, Y., Hu, L., Chen, Z., Sun, F., et al. (2021). A case study of 10 years groundwater radon monitoring along the eastern margin of the Tibetan Plateau and in its adjacent regions: implications for earthquake surveillance. *Appl. Geochem.* 131, 105014. doi:10.1016/j.apgeochem.2021.105014

Zheng, G., Martinelli, G., Wang, Y., Li, S., and Ma, X. (2022). Notes for a history of gas geochemistry. *J. Asian Earth Sci.* 33 (6), 1614–1623. doi:10.1007/s12583-022-1758-2

Zheng, G., Xu, S., Liang, S., Shi, P., and Zhao, J. (2013). Gas emission from the Qingzhu river after the 2008 Wenchuan earthquake, Southwest China. *Chem. Geol.* 339, 187–193. doi:10.1016/j.chemgeo.2012.10.032

Zheng, G., Xu, W., Etiope, G., Ma, X., Liang, S., Fan, Q., et al. (2018). Hydrocarbon seeps in petroliferous basins in China: a first inventory. *J. Asian Earth Sci.* 151, 269–284. doi:10.1016/j.jseaes.2017.10.037

Zhou, X., Chen, Z., and Cui, Y. (2016). Environmental impact of CO_2, Rn, Hg degassing from the rupture zones produced by Wenchuan M_S8.0 earthquake in western Sichuan, China. *Environ. Geochem. Health.* 38 (5), 1067–1082. doi:10.1007/s10653-015-9773-1

Zondervan, J. R., Hilton, R. G., Dellinger, M., Clubb, F. J., Roylands, T., and Ogric, M. (2023). Rock organic carbon oxidation CO_2 release offsets silicate weathering sink. *Nature* 623 (7986), 329–333. doi:10.1038/s41586-023-06581-9